

BRIEF REPORT

Coherent Structural and Functional Network Changes after Thalamic Lesions in Essential Tremor

Emily D.R. Pohl,¹ Neeraj Upadhyay, PhD,¹ Xenia Kobeleva, MD,^{2,3} Veronika Purrer, MD,^{2,3} Angelika Maurer, MSc,^{1,3} Vera C. Keil, MD,^{4,5} Christine Kindler, MD,^{2,3} Valeri Borger, MD,⁶ Claus C. Pieper, MD,⁷ Simon Groetz, MD,⁴ Lukas Scheef, MD,¹ Jaroslaw Maciacyk, MD,^{8,9} Hans Schild, MD,⁷ Hartmut Vatter, MD,⁶ Thomas Klockgether, MD,^{2,3} Alexander Radbruch, MD, JD,^{3,4} Ulrike Attenberger, MD,⁷ Ullrich Wüllner, MD, PhD,^{2,3} and Henning Boecker, MD^{1,3*}

¹Division "Clinical Functional Imaging," Department of Diagnostic and Interventional Radiology, University Hospital Bonn, Bonn, Germany ²Department of Neurology, University Hospital Bonn, Bonn, Germany ³German Center for Neurodegenerative Diseases (DZNE), Bonn, Germany ⁴Department of Neuroradiology, University Hospital Bonn, Bonn, Germany ⁵Department of Radiology and Nuclear Medicine, Amsterdam UMC, VUmc, Amsterdam, the Netherlands ⁶Department of Neurosurgery, University Hospital Bonn, Bonn, Germany ⁷Department of Diagnostic and Interventional Radiology, University Hospital Bonn, Bonn, Germany ⁸Stereotactic and Functional Neurosurgery, Department of Neurosurgery, University Hospital Bonn, Bonn, Germany ⁹Division of Neurosurgery, Department of Surgical Sciences, Dunedin School of Medicine, University of Otago, Dunedin, New Zealand

ABSTRACT: Background: Magnetic resonance-guided focused ultrasound of the ventral intermediate nucleus is a novel incisionless ablative treatment for essential tremor (ET).

Objective: The aim was to study the structural and functional network changes induced by unilateral sonication of the ventral intermediate nucleus in ET.

Methods: Fifteen essential tremor patients (66.2 ± 15.4 years) underwent probabilistic tractography and functional magnetic resonance imaging (MRI) during unilateral postural tremor-eliciting tasks using 3-T MRI

before, 1 month ($N = 15$), and 6 months ($N = 10$) post unilateral sonication.

Results: Tractography identified tract-specific alterations within the dentato-thalamo-cortical tract (DTCT) affected by the unilateral lesion after sonication. Relative to the treated hand, task-evoked activation was significantly reduced in contralateral primary sensorimotor cortex and ipsilateral cerebellar lobules IV/V and VI, and vermis. Dynamic causal modeling revealed a significant decrease in excitatory drive from the cerebellum to the contralateral sensorimotor cortex.

Conclusions: Thalamic lesions induced by sonication induce specific functional network changes within the DTCT, notably reducing excitatory input to ipsilateral sensorimotor cortex in ET. ©[2022] International Parkinson and Movement Disorder Society. © 2022 The Authors. *Movement Disorders* published by Wiley Periodicals LLC on behalf of International Parkinson and Movement Disorder Society

Key Words: essential tremor; magnetic resonance imaging; brain networks; magnetic resonance-guided focused ultrasound; ventral intermediate nucleus

Abbreviations

CTCC	cerebello-thalamo-cortical circuit
DBS	deep brain stimulation
DCM	dynamic causal modeling
DTCT	dentato-thalamo-cortical tract
DTI	diffusion tensor imaging
ET	essential tremor
FA	fractional anisotropy
fMRI	functional magnetic resonance imaging
FTM	Fahn–Tolosa–Marin Clinical Rating Scale for tremor
FWE	family-wise error
M1	primary motor cortex
MRgFUS	magnetic resonance-guided focused ultrasound
MRI	magnetic resonance imaging
ROI	region of interest
VIM	ventral intermediate nucleus

This is an open access article under the terms of the [Creative Commons Attribution](#) License, which permits use, distribution and reproduction in any medium, provided the original work is properly cited.

*Correspondence to: Dr. Henning Boecker, Department of Diagnostic and Interventional Radiology, University Hospital Bonn, Venusberg-Campus 1, D-53127 Bonn, Germany; E-mail: henning.boecker@ukbonn.de

Emily D.R. Pohl, Neeraj Upadhyay, and Xenia Kobeleva share first authorship.

Relevant conflicts of interest/financial disclosures: The authors declare no conflicts of interest related to this study.

Funding agency: The MRgFUS facility was funded by the German Research Foundation (INST 1172/64-1).

Received: 3 March 2022; **Revised:** 2 May 2022; **Accepted:** 1 June 2022

Published online in Wiley Online Library (wileyonlinelibrary.com). DOI: 10.1002/mds.29130

Essential tremor (ET) manifests as a postural and/or kinetic limb tremor that can be medically refractory and require stereotactic treatment.^{1,2} The thalamic ventral intermediate nucleus (VIM) is an established target for different stereotactic procedures in ET, including deep brain stimulation (DBS) and, more recently, magnetic resonance-guided focused ultrasound (MRgFUS). MRgFUS utilizes ultrasonic waves for incisionless high-precision ablation of brain target sites.³⁻⁵ Clinical improvement after VIM MRgFUS treatment has been validated meta-analytically,⁶ and studies have shown long-term tremor suppression and quality-of-life improvements similar to DBS.⁷⁻¹⁰

ET is considered to result from neuronal oscillations,¹¹⁻¹³ and the “oscillating network hypothesis”¹³ postulates oscillatory activity within the cerebello-thalamo-cortical circuits (CTCC).¹⁴ Within this network, the VIM constitutes a “cerebellar receiving area” projecting its output toward the ipsilateral primary motor cortex (M1)¹⁵⁻¹⁷ via the dentato-thalamo-cortical tract (DTCT).¹⁸⁻²⁰

To unravel network changes induced by unilateral VIM MRgFUS treatment, we performed a longitudinal magnetic resonance imaging (MRI) study in 15 ET patients: functional magnetic resonance imaging (fMRI) was performed before, 1 month ($N = 15$), and 6 months ($N = 10$) post unilateral VIM MRgFUS treatment to examine (1) blood-oxygenation-level-dependent signal changes during unilateral forearm elevations and (2) modeling-directed network properties within the CTCC. Diffusion tensor imaging (DTI) and probabilistic tractography were applied to delineate the DTCT, and whole-brain voxel-based analyses of fractional anisotropy (FA) was used to visualize associated microstructural changes.

Patients and Methods

Patients

For details on study registry and ethics, see Supplementary Data.

Patients aged ≥ 18 years diagnosed with definite medication-refractory ET² were included. Patients with marked head tremor and/or other movement disorders were excluded. Patients' demographics, including age, handedness, duration of tremor, alcohol sensitivity, family history, and medication history, were recorded. On each of the four MRI examination days (or the day before), tremor was rated using the Fahn–Tolosa–Marin Clinical Rating Scale for tremor (FTM)^{21,22} (see Supplementary Data).

Stereotactic Intervention

MRgFUS of contralateral VIM was performed for the treatment of 14 right-handed patients and 1 left-handed patient (for details, see Supplementary Data).

Statistical Analyses of Clinical Data

Clinical data were analyzed using SPSS 28 (SPSS Inc., Chicago, IL). Normal distribution was verified using Shapiro–Wilk test. Most, but not all, data were normally distributed. Simulation studies have shown that paired t tests and the repeated measures analyses of variance (ANOVAs) are relatively robust to normal distribution assumption violations,²³ especially if no further assumption is violated.²⁴ Therefore, data were processed using parametric tests. For the FTM, two ANOVAs were calculated: (1) 2 (time: before/1-month post MRgFUS) \times 2 (side: treated/untreated) and (2) 2 (time: before/6-month post-MRgFUS) \times 2 (side: treated/untreated). Post hoc, paired t tests were performed. P -values < 0.05 were regarded as statistically significant. Effect sizes are reported as partial eta squared (η_p^2) for ANOVAs and Cohens' d for post hoc tests. Data are presented as mean \pm standard deviation.

MRI Procedures

MRI Acquisition

T1-weighted images, task fMRI, and DTI were performed on a 3T-MRI System (Philips Healthcare, Best, the Netherlands) equipped with an eight-channel head coil.

fMRI Task

Task-fMRI examinations were performed 1 or 2 days before and subsequently 3 days, 1 month, and 6 months post MRgFUS. Here we report only the 1- and 6-month data, when local edema had faded²⁵ and clinical effects were robust. Postural tremor was elicited by forearm elevations followed by resting phases (Fig. APPENDIX S1; see Supplementary Data).

MRI Analyses

Details of the methods of MRI acquisition and fMRI-, dynamic causal model (DCM)- and DTI analyses are provided in the Supplementary Data.

Results

Clinical

Patients

Of 21 included patients, $N = 4$ were excluded due to imaging artifacts, $N = 1$ due to false DTI acquisition, and $N = 1$ due to missing data, resulting in a final sample size of $N = 15$ for 1-month post follow-up. At 6-month follow-up, $N = 5$ patients dropped out, $N = 2$ lost interest, $N = 2$ dropped out due to COVID pandemic restrictions, and $N = 1$ dropped out after receiving a metal implant.

Patient demographics were as follows: males/females: 12/3; lesion left/right: 14/1; mean age: 66.2 ± 15.4 years;

mean skull density ratio: 0.45 ± 0.1 ; disease duration: 31.7 ± 11.0 years; age of onset: 34.5 ± 16.5 years; family history: positive in 80.0%. For detailed demographical and clinical information, see Table APPENDIX S1.

Side Effects

The side effects of the MRgFUS treatment within the follow-up period of 6 months included involuntary movements, taste disturbance, dysmetria, subjective unsteadiness, objective ataxia, and paresthesia (Table S2).

Fahn–Tolosa–Marin Clinical Rating Scale for Tremor

Clinical Change in Tremor (AB Score) at 1-Month Follow-Up. The results of the ANOVA in 15 ET patients revealed a significant main effect of time ($F(1, 14) = 48.3$; $P < 0.001$; $\eta_p^2 = 0.775$), a significant main effect of side ($F(1, 14) = 71.3$; $P < 0.001$; $\eta_p^2 = 0.836$), and a significant time-by-side interaction ($F(1, 14) = 142.9$; $P < 0.001$; $\eta_p^2 = 0.911$).

Post hoc tests: as shown in Figure S2, subscore AB for the treated upper extremity showed a significant decrease from before to 1-month post MRgFUS (by $78.7 \pm 11.5\%$; ($t(14) = 11.1$; $P < 0.001$; $d = 2.87$). For the untreated side no significant change (increase by $5.8 \pm 28.5\%$) was detected ($t(14) = -0.55$; $P = 0.589$; $d = -0.14$). Comparison between both sides showed that the decrease in the treated side was significantly larger ($t(14) = 11.96$; $P < 0.001$; $d = 3.09$).

Clinical Change in Tremor (AB Score) at 6-Month Follow-Up. Findings were similar to 1-month data, indicating a stable clinical effect. The results of the ANOVA for AB score after 6 months and paired t tests for total FTM score and subscores A, B (treated and untreated), and C are reported in Supplementary Data. Individual tremor scores are presented in Table S3.

Imaging Findings

Task-fMRI Data

Analysis of task-fMRI data for treated and untreated side before, 1-month, and 6-month post MRgFUS revealed typical activation clusters during tremor-eliciting arm elevations (Fig. S3; Tables S4 and S5).

ANOVA for analysis before versus 1-month post MRgFUS revealed a significant main effect of time and side but no significant time-by-side interaction (Fig. S4A,B). A significant reduction in activation from before to 1-month post MRgFUS was exclusively found for the treated hand in contralateral M1, contralateral primary sensory cortex and the lobules IV/V and VI, and vermis of the ipsilateral cerebellum ($P < 0.001$,

corrected for family-wise error [FWE] with cluster threshold $k = 105$; Fig. 1A; Table S6). In addition, β -weights extracted from two regions of interest (ROIs), M1-ROI and cerebellum ROI, decreased from before to 1-month post MRgFUS for the treated arm (Fig. 1C) but not for the untreated arm. An increase in activation was found before to 1-month post MRgFUS in posterior cingulate cortex/precuneus and angular/parietal inferior gyrus ($P < 0.001$, corrected for FWE with cluster threshold $k = 61$; Fig. S5).

The results were replicated in the 2×2 ANOVA for timepoints before versus 6-month post MRgFUS (Fig. 1B,D; Figures S6 and S7; Table S7). In addition, a significant time-by-side interaction was found in bilateral precuneus and bilateral cingulate gyrus (Fig. S6C).

Finally, subgroup analysis ($N = 10$), including all three timepoints (2×3 ANOVA), further supported results from both 2×2 ANOVAs (Fig. S8).

Dynamic Causal Modeling Data

MRgFUS led to substantial changes in long-range connections between M1 and the cerebellum (Fig. S9C, D). Excitatory connections from the cerebellum to M1 were reduced at 1- and 6-month post MRgFUS, and excitatory connections from M1 to the cerebellum were increased at 1-month post MRgFUS (compared to pre MRgFUS). All group contrasts had posterior probabilities $>95\%$, indicating a strong effect.

Fiber Tract and Microstructural Integrity Data

Probabilistic tractography showed the lesion to affect the DTCT on its route to the contralateral M1 handknob area (Fig. 2A,B), where a significant reduction in task-fMRI activation was found. DTCT streamline counts were reduced at 1-month post MRgFUS (Fig. 2C) in $N = 13$ subjects ($t(12) = -3.82$, $P_{2-tailed} = 0.002$) and at 6-month post MRgFUS (Fig. 2D) in $N = 9$ subjects ($t(8) = -2.48$, $P_{2-tailed} = 0.038$) amenable to streamline analyses (Table S8).

Local FA reduction within the DTCT is shown in Figure S10. A voxel-wise whole-brain level within subject-repeated measures ANOVA identified FA changes within the thalamus near the lesion ($k = 25$). Post hoc comparisons revealed that FA changes were significant only at 1-month post MRgFUS. For individual FA values before, 1-month and 6-month post MRgFUS, see Table S8.

Discussion

To the best of our knowledge, this is the first study in ET investigating structural and functional effects within the CTCC after unilateral VIM MRgFUS. The lesion was located within the DTCT. Streamline counts in the DTCT were significantly reduced, indicating disruption

Functional MRI Group Analysis

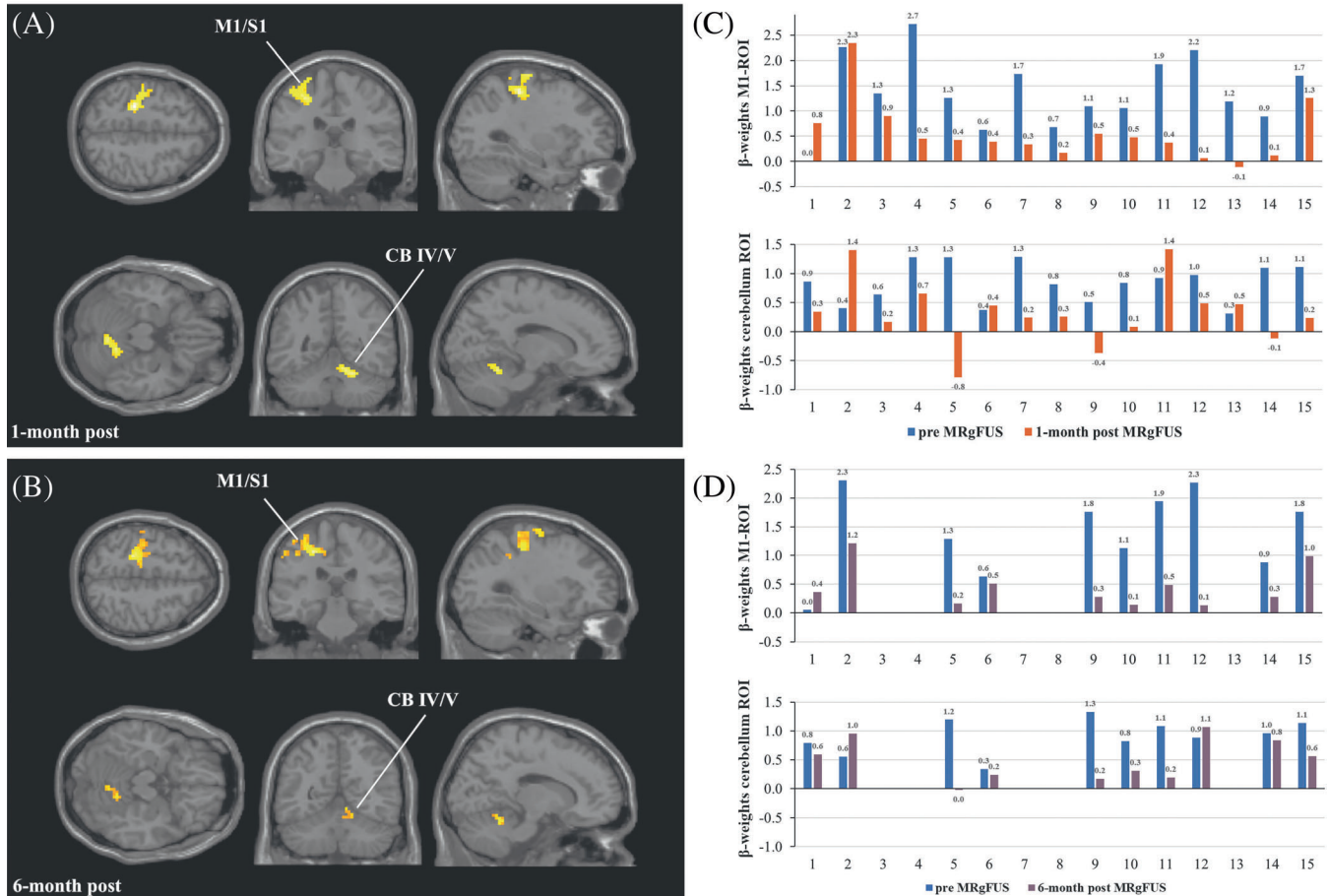


FIG. 1. fMRI group analysis: reduced activation of contralateral sensorimotor cortex and ipsilateral cerebellum (left); visualization of β -weights extracted from M1-ROI and cerebellum-ROI (right); **(A)** contrast pre MRgFUS versus 1-month post MRgFUS; N = 15; **(B)** contrast pre MRgFUS versus 6-month post MRgFUS; N = 10; **(C)** β -weights pre MRgFUS versus 1-month post MRgFUS; N = 15; **(D)** β -weights pre MRgFUS versus 6-month post MRgFUS; N = 10. Abbreviations: CB, cerebellum; CB IV/CB V, cerebellar lobules IV and V; M1, primary motor cortex; ROI, region of interest, S1, primary sensory cortex; fMRI, functional magnetic resonance imaging; MRgFUS, magnetic resonance-guided focused ultrasound. [Color figure can be viewed at wileyonlinelibrary.com]

of fiber connectivity. Reductions in FA were found within the tract (adjacent to the lesion) at 1-month post MRgFUS, indicating local tract-specific disruption of fiber microstructural integrity. Activation decreases were observed in contralateral primary sensorimotor cortex, ipsilateral cerebellar lobules IV/V and VI, and vermis (IV/V and VI). DCM analyses in the tremor network (informed by Buijink and colleagues²⁶) found sustained reductions in excitatory drive from ipsilateral cerebellum to contralateral M1 at both timepoints.

Findings indicate long-range effects in the tremor network extending beyond the local VIM target that converge in the precentral gyrus and are in line with in vivo tractography data in ET patients, showing M1 as terminal thalamo-cortical projection of the DTCT.¹⁸⁻²⁰ The thalamo-cortical projections from the VIM nucleus to M1 are glutamatergic,^{27,28} and similarly, DCM analyses found reductions in excitatory drive from the cerebellum to M1. Moreover, significant reductions in task-evoked

activity were found post-MRgFUS in ipsilateral sensorimotor cerebellum. Given that the VIM is innervated by excitatory glutamatergic projections from the dentate nucleus,²⁸⁻³⁰ findings hint at normalization of pathological network overactivity. DCM analysis also informed about increased excitatory input from M1 to cerebellar lobules V and VIII at 1 month post-MRgFUS. This is an interesting observation, as activation increases were also reported during rest in cerebellar lobule V after DBS of the zona incerta.³¹

In summary, functional changes post-MRgFUS were identified in contralateral M1, along with micro- and macrostructural alterations within the affected DTCT. Based on these data, we propose a network model in which altered fiber connections from the cerebellum to M1 following VIM MRgFUS reduce excitatory drive from the cerebellum to M1. Remote changes in cerebellar activity hint at a normalization of previously aberrant activity within the CTCC.

DTI Analysis

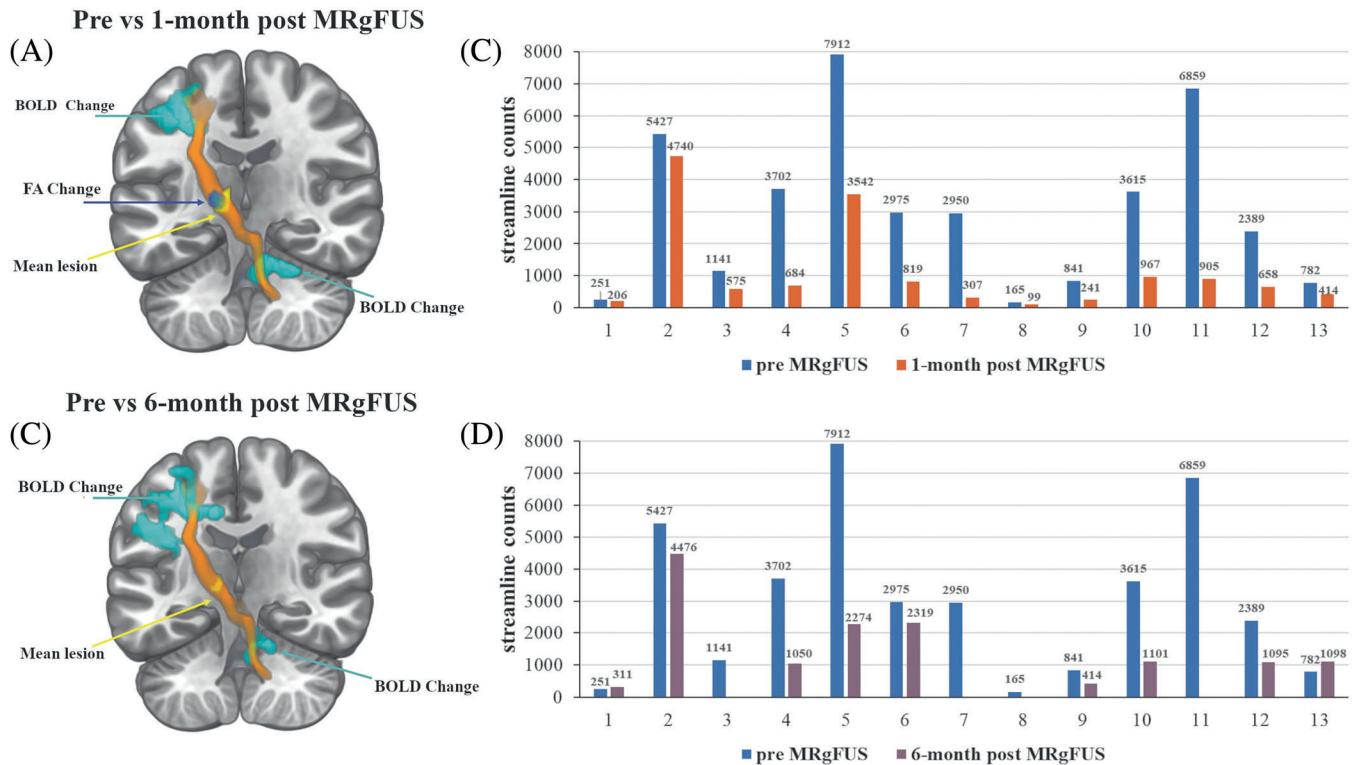


FIG. 2. DTI analysis: a qualitative presentation of the BOLD and DTI changes: (A) 1-month and (B) 6-month post MRgFUS, showing lesion (yellow), fractional anisotropy decrease (blue), BOLD decrease (turquoise), and within group-averaged dentato-thalamo-cortical tract (orange) for respective time points; visualization of streamline counts is presented in (C) pre (blue) and 1-month (orange) and (D) pre (blue) and 6-month (purple) post MRgFUS. Abbreviations: BOLD, blood-oxygenation-level-dependent; DTI, diffusion tensor imaging; FA, fractional anisotropy. [Color figure can be viewed at wileyonlinelibrary.com]

As limitations, we acknowledge that DCM is a model-based procedure based on certain assumptions and that in our study the estimation of the model relies on measures of blood flow changes instead of direct neural recordings. Further studies applying neuromodulative procedures might be used to confirm our assumptions and to draw causal interferences on cerebello-cerebral circuit function. Furthermore, we acknowledge the small sample size, $N = 10$ patients, at 6 months for functional analyses. It would be advantageous to conduct further longitudinal multimodal imaging studies in larger ET cohorts after MRgFUS to gain further insights into the functional and structural effects of MRgFUS. ■

Acknowledgments: We are grateful to the patients for their participation in this study. Open Access funding enabled and organized by Projekt DEAL.

Data Availability Statement

The data that support the findings of this study are available on request from the corresponding author. The data are not publicly available due to privacy or ethical restrictions.

REFERENCES

- Picillo M, Fasano A. Recent advances in essential tremor: surgical treatment. *Parkinsonism Relat Disord* 2016;22(Suppl 1):S171–S175.
- Bhatia KP, Bain P, Bajaj N, et al. Consensus statement on the classification of tremors. From the task force on tremor of the International Parkinson and Movement Disorder Society. *Mov Disord* 2018;33(1):75–87.
- Jagannathan J, Sanghvi NT, Crum LA, et al. High-intensity focused ultrasound surgery of the brain: part 1—a historical perspective with modern applications. *Neurosurgery* 2009;64(2):201–210. discussion 210–201.
- Boutet A, Ranjan M, Zhong J, et al. Focused ultrasound thalamotomy location determines clinical benefits in patients with essential tremor. *Brain* 2018;141(12):3405–3414.
- Kapadia AN, Elias GJB, Boutet A, et al. Multimodal MRI for MRgFUS in essential tremor: post-treatment radiological markers of clinical outcome. *J Neurol Neurosurg Psychiatry* 2020;91(9):921–927.
- Mohammed N, Patra D, Nanda A. A meta-analysis of outcomes and complications of magnetic resonance-guided focused ultrasound in the treatment of essential tremor. *Neurosurg Focus* 2018;44(2):E4.
- Chang JW, Park CK, Lipsman N, et al. A prospective trial of magnetic resonance-guided focused ultrasound thalamotomy for essential tremor: results at the 2-year follow-up. *Ann Neurol* 2018;83(1):107–114.
- Harary M, Segar DJ, Hayes MT, Cosgrove GR. Unilateral thalamic deep brain stimulation versus focused ultrasound Thalamotomy for essential tremor. *World Neurosurg* 2019;126:e144–e152.

9. Langford BE, Ridley CJA, Beale RC, Caseby SCL, Marsh WJ, Richard L. Focused ultrasound Thalamotomy and other interventions for medication-refractory essential tremor: an indirect comparison of short-term impact on health-related quality of life. *Value Health* 2018;21(10):1168–1175.
10. Elias WJ, Lipsman N, Ondo WG, et al. A randomized trial of focused ultrasound Thalamotomy for essential tremor. *N Engl J Med* 2016;375(8):730–739.
11. Llinas RR. The intrinsic electrophysiological properties of mammalian neurons: insights into central nervous system function. *Science* 1988;242(4886):1654–1664.
12. Madelein van der Stouwe AM, Nieuwhof F, Helmich RC. Tremor pathophysiology: lessons from neuroimaging. *Curr Opin Neurol* 2020;33(4):474–481.
13. Helmich RC, Toni I, Deuschl G, Bloem BR. The pathophysiology of essential tremor and Parkinson's tremor. *Curr Neurol Neurosci Rep* 2013;13(9):378.
14. Raethjen J, Deuschl G. The oscillating central network of essential tremor. *Clin Neurophysiol* 2012;123(1):61–64.
15. Hyam JA, Owen SL, Kringelbach ML, et al. Contrasting connectivity of the ventralis intermedius and ventralis oralis posterior nuclei of the motor thalamus demonstrated by probabilistic tractography. *Neurosurgery* 2012;70(1):162–169. discussion 169.
16. Macchi G, Jones EG. Toward an agreement on terminology of nuclear and subnuclear divisions of the motor thalamus. *J Neurosurg* 1997;86(4):670–685.
17. Krack P, Dostrovsky J, Ilinsky I, et al. Surgery of the motor thalamus: problems with the present nomenclatures. *Mov Disord* 2002;17(Suppl 3):S2–S8.
18. Akram H, Dayal V, Mählknecht P, et al. Connectivity derived thalamic segmentation in deep brain stimulation for tremor. *Neuroimage Clin* 2018;18:130–142.
19. Ezponda A, Calvo-Imirizaldu M, Malmierca P, et al. Mapping the Cortical Connections of the Ventral Intermediate Nucleus (VIM) with Tractography in Patients Undergoing MRI-Guided High Intensity Focused Ultrasound (HIFU) Thalamotomy. *Radiological Society of North America. RSNA, 105th Scientific Assembly and Annual Meeting, Chicago; 2019.*
20. Klein JC, Barbe MT, Seifried C, et al. The tremor network targeted by successful VIM deep brain stimulation in humans. *Neurology* 2012;78(11):787–795.
21. TE Fahn S, Marin C. Clinical rating scale for tremor. In: TE JJ, ed. *Parkinson's Disease and Movement Disorders*. 2nd ed. Baltimore, MD: Williams & Wilkins; 1993:225–234.
22. Elble R, Bain P, Forjaz MJ, et al. Task force report: scales for screening and evaluating tremor: critique and recommendations. *Mov Disord* 2013;28(13):1793–1800.
23. Vasey MW, Thayer JF. The continuing problem of false positives in repeated measures ANOVA in psychophysiology: a multivariate solution. *Psychophysiology* 1987;24(4):479–486.
24. Berkovits I, Hancock GR, Nevitt J. Bootstrap resampling approaches for repeated measure designs: relative robustness to Sphericity and normality violations. *Educ Psychol Meas* 2000;60(6):877–892.
25. Keil VC, Borger V, Purrer V, et al. MRI follow-up after magnetic resonance-guided focused ultrasound for non-invasive thalamotomy: the neuroradiologist's perspective. *Neuroradiology* 2020;62(9):1111–1122.
26. Buijink AW, van der Stouwe AM, Broersma M, et al. Motor network disruption in essential tremor: a functional and effective connectivity study. *Brain* 2015;138(Pt 10):2934–2947.
27. Rouiller EM, Liang F, Babalian A, Moret V, Wiesendanger M. Cerebellothalamocortical and pallidothalamocortical projections to the primary and supplementary motor cortical areas: a multiple tracing study in macaque monkeys. *J Comp Neurol* 1994;345(2):185–213.
28. Milosevic L, Kalia SK, Hodaie M, Lozano AM, Popovic MR, Hutchison WD. Physiological mechanisms of thalamic ventral intermediate nucleus stimulation for tremor suppression. *Brain* 2018;141(7):2142–2155.
29. Asanuma C, Thach WT, Jones EG. Distribution of cerebellar terminations and their relation to other afferent terminations in the ventral lateral thalamic region of the monkey. *Brain Res* 1983;286(3):237–265.
30. Anderson ME, Turner RS. Activity of neurons in cerebellar-receiving and pallidal-receiving areas of the thalamus of the behaving monkey. *J Neurophysiol* 1991;66(3):879–893.
31. Awad A, Blomstedt P, Westling G, Eriksson J. Deep brain stimulation in the caudal zona incerta modulates the sensorimotor cerebello-cerebral circuit in essential tremor. *Neuroimage* 2020;209:116511.

Supporting Data

Additional Supporting Information may be found in the online version of this article at the publisher's web-site.

SGML and CITI Use Only DO NOT PRINT

Author Roles

E.D.R.P. contributed to data acquisition, analysis, and interpretation; drafted the manuscript; and critically revised the manuscript.

N.U. contributed to analysis and interpretation, drafted the manuscript, and critically revised the manuscript.

X.K. contributed to analysis and interpretation, drafted the manuscript, and critically revised the manuscript.

V.P. contributed to data acquisition and critically revised the manuscript.

A.M. contributed to analysis and interpretation, drafted the manuscript, and critically revised the manuscript.

V.C.K. contributed to data acquisition and critically revised the manuscript.

C.K. contributed to data acquisition and critically revised the manuscript.

V.B. contributed to data acquisition and critically revised the manuscript.

C.C.P. contributed to data acquisition and critically revised the manuscript.

S.G. contributed to data acquisition and critically revised the manuscript.

J.M. contributed to data acquisition and critically revised the manuscript.

H.S. contributed to infrastructure, data acquisition, and critical revision of the manuscript.

H.V. contributed to conception and design and critically revised the manuscript.

T. K. contributed to conception and design and critically revised the manuscript.

L.S. contributed to conception, design, and data acquisition and critically revised the manuscript.

A.R. contributed to infrastructure and critically revised the manuscript.

U.A. contributed to infrastructure and critically revised the manuscript.

U.W. contributed to conception, design, and data acquisition and critically revised the manuscript.

H.B. contributed to conception, design, analysis, and data interpretation and drafted and critically revised the manuscript.

All authors provided their final approval and are accountable for all aspects of the work in ensuring that questions related to the accuracy or integrity of any part of the work are appropriately investigated and resolved.

Full financial disclosures for the previous 12 months

T.K. receives research support from the Bundesministerium für Bildung und Forschung (BMBF), the National Institutes of Health (NIH), and Servier. Within the past 24 months, he has received consulting fees from Biogen, UCB, and Vico Therapeutics.

A.R. receives study support from Bayer Health Care and Guerbet.

C.C.P. receives grant support from Guerbet; Speakers Bureau: Guerbet, Philips Healthcare, and Bayer Vital.

H.B. receives grant support from the BONFOR program of the University of Bonn and royalties from Springer.